

蒋莹, 韦唯, 冯小艺, 等. 过去64万年以来湖北三宝洞石笋生长速率变化及其古气候意义[J]. 中国岩溶, 2023, 42(3): 582-589.  
DOI: 10.11932/karst2021y31

# 过去64万年以来湖北三宝洞石笋生长速率变化及其古气候意义

蒋莹<sup>1,2</sup>, 韦唯<sup>1</sup>, 冯小艺<sup>1</sup>, 张晗<sup>1</sup>, 朱和<sup>1</sup>, 董进国<sup>1</sup>

(1. 南通大学地理科学学院, 江苏南通 226006; 2. 南京师范大学地理科学学院, 江苏南京 210023)

**摘要:** 利用石笋平均生长速率变化来重建古气候环境变迁已成为洞穴古气候研究的重要领域。文章以湖北三宝洞横跨22~64万年的5支石笋167个<sup>230</sup>Th年龄数据为材料, 结合过去的工作, 重建了晚更新世64万年以来长江中下游地区东亚夏季风降水变化过程。结果表明: 深海氧同位素(MIS)1,5,3,5.5,7.3,7.5,9,15.1,15.5阶段石笋生长速率显著增大, 指示东亚夏季风强度增强, 降水增多; 相反, 冰期阶段生长速率缓慢或者不发育, 指示夏季风强度减弱, 降水明显减少, 但平均生长速率指标并不能定量指示夏季风强度变化。当石笋生长速率低于 $10\mu\text{m}\cdot\text{a}^{-1}$ 时, 不能有效地指示冰期—间冰期旋回变化。在轨道尺度上, 平均生长速率所揭示的冰期—间冰期波动可能归因于全球冰量和太阳辐射共同作用的结果。

**关键词:** 石笋; 生长速率; 冰期—间冰期; 东亚夏季风; 三宝洞; 湖北

**中图分类号:** P532; P931 **文献标识码:** A

**文章编号:** 1001-4810(2023)03-0582-08

开放科学(资源服务)标识码(OSID):



## 0 引言

近年来, 石笋平均生长速率常被作为反映古气候、古环境变化的有效代用指标<sup>[1-3]</sup>, 用来描述石笋发育特征, 恢复不同区域环境气候变化历程<sup>[4]</sup>。例如杨琰等<sup>[5]</sup>对贵州荔波董歌洞较老(>250 ka)石笋的135个<sup>230</sup>Th年龄数据及生长速率研究得出, 石笋生长速率在间冰期处于高值, 在冰期处于低值, 在间冰期和冰期转化阶段呈现跳跃式变化; 张美良等<sup>[6]</sup>对广西桂林盘龙洞石笋沉积速率动态监测发现, 新碳酸盐的主要沉积时段发生在夏半年, 旱季(或冬季)平均沉积量最小, 表现出雨热同季的季节变化和年际变化的特点; 董进国<sup>[7]</sup>利用湖北三宝洞17支石笋190个年代测试点统计分析了过去22万年以来石笋

平均生长速率的变化过程, 结果发现: 在冰期, 石笋平均生长速率缓慢; 相反在间冰期, 石笋平均生长速率快。石笋平均生长速率在轨道尺度上可以反映东亚夏季风强度的变化<sup>[7-8]</sup>。然而, 在不同时间尺度上, 石笋生长速率变化控制因素较为复杂, 洞穴内部环境差异所产生的噪音有可能掩盖或削弱洞穴外部气候信号在洞穴内部的表达。例如, 何潇等<sup>[9]</sup>利用重庆地区梁天湾洞和水鸣洞石笋生长速率数据, 结合氧同位素数据, 分析发现石笋生长速率最快的时期并不总是氧同位素最偏轻、气候最湿润的阶段; 南京葫芦洞<sup>[3]</sup>石笋生长速率数据显示, 在深海洋同位素(MIS)2阶段与3阶段, 生长速率明显增加, 而同期湖北三宝洞<sup>[7]</sup>的石笋生长速率则明显降低, 甚至停止生长。因此, 利用石笋平均生长速率重建古环境

基金项目: 国家自然科学基金项目(41877287, 41472317, 41102216); 江苏省大学生创新项目(201910304116Y)

第一作者简介: 蒋莹(2000—), 女, 硕士, 研究方向为第四纪环境演变。E-mail: 2231472188@qq.com。

通信作者: 董进国(1978—), 男, 博士, 教授, 主要从事第四纪年代学与环境演变专业。E-mail: dongjinguo1111@163.com。

收稿日期: 2021-03-20

较为复杂,需谨慎对待。考虑到湖北三宝洞在末次冰期期间石笋生长并不连续,本文利用湖北三宝洞最近发表的 5 支石笋样品<sup>[10]</sup>,结合过去的工作<sup>[7]</sup>,将石笋生长时间序列从过去 22 万年延伸至 64 万年,进一步评估石笋平均生长速率在轨道尺度上的变化特征及其所指示的古气候意义。

## 1 研究区域概况

湖北神农架自然保护区位于长江三峡段北岸,与黄土高原南缘相邻,主要受东亚夏季风的影响。该区域年均温为 8~9 °C,年均降水量为 2 000 mm。夏季,来自赤道大洋的暖湿气流进入大陆腹地,带来约 60% 的年降水量;冬季,来自西伯利亚的干冷气团控制了神农架地区的气候。因此,该地区对东亚夏季风的季节性进退变化特别敏感。三宝洞海拔 1 900 m,位于湖北神农架山脉的北坡上,覆盖着厚约 300 m 的石灰岩层。表层土壤层厚 2~3 m,主要生长着乔木、灌木和杂草等。

## 2 材料和方法

本文研究的 5 支石笋(编号为: SB12、SB14、SB32、SB58、SB61)均来自湖北三宝洞,累计高度约为 2.991 m,其中,SB61 沉积于 229.4~384 ka B.P.,对应于 MIS8~MIS10; SB14 生长发育于 299.6~622.8 ka B.P.,从 MIS9 横跨至 MIS15; SB12、SB58 分别沉积于 425.1~462.7 ka B.P. 与 426.7~464.7 ka B.P.,对应于 MIS12; SB32 生长于 514.3~638.2 ka B.P.,从 MIS13 横跨至 MIS15。5 支石笋共获得 167 个<sup>230</sup>Th 年龄数据(表 1),分析仪器为 Thermo-Finnigan Element 和 Thermo-Finnigan Neptune,由美国明尼苏达同位素实验室完成,年龄分析误差为 $\pm 2\sigma$  测量统计误差,误差精度在 0.5~2.0 ka。计算石笋平均生长速率,首先剔除地层学中石笋年龄倒转的数据;然后建立石笋实测年龄点及相应的生长深度曲线(图 1),新的结果与原始文献中生长速率<sup>[10]</sup> 曲线基本一致;最后由相邻两点深度差除以实测年龄差得出石笋平均生长速率。

## 3 结果与分析

从图 1 石笋年龄—深度曲线来看,石笋

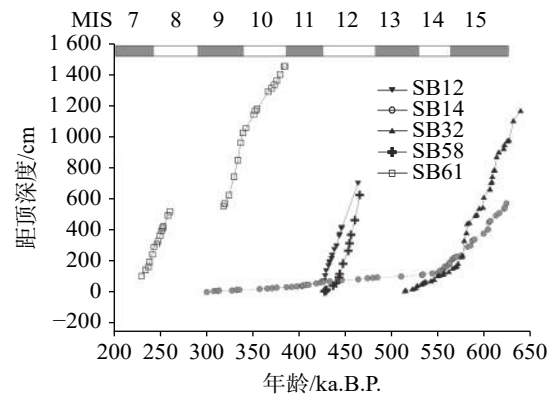


图 1 石笋年龄—深度曲线图

图中数字代表深海氧同位素阶段,灰色条带表示间冰期,白色条带代表冰期

Fig. 1 Curve of the age-depth models for five stalagmites in Sanbao cave

(The number refers to marine isotope stages; the gray strip refers to interglacial stage; the white strip refers to glacial stage)

SB61 发育并不连续,存在一个明显的沉积间断。在 229.4~260 ka B.P. 和 317.7~384.2 ka B.P. 两个连续生长段,其生长速率在  $6\sim 32 \mu\text{m}\cdot\text{a}^{-1}$  之间波动,平均约为  $14 \mu\text{m}\cdot\text{a}^{-1}$ ; 石笋 SB14 持续生长时间最长,跨越了约 300 ka,但其平均生长速率极其缓慢,尤其是在 540 ka B.P. 之后,其平均生长速率低于  $1 \mu\text{m}\cdot\text{a}^{-1}$ 。在此之前生长速率有所增加,但绝大多数(约占 86%) 在  $1.5\sim 9 \mu\text{m}\cdot\text{a}^{-1}$  之间波动。2 支石笋(SB12、SB58) 沉积于相同生长时段(表 1),其生长速率大体相近,在  $4\sim 46 \mu\text{m}\cdot\text{a}^{-1}$  之间波动,平均生长速率分别为  $18 \mu\text{m}\cdot\text{a}^{-1}$  和  $16 \mu\text{m}\cdot\text{a}^{-1}$ 。石笋 SB32 在 514.3~638.2 ka B.P. 期间连续沉积,在 575 ka B.P. 之前,其生长速率变化较大,在  $1.4\sim 60 \mu\text{m}\cdot\text{a}^{-1}$  之间波动,平均生长速率为  $21 \mu\text{m}\cdot\text{a}^{-1}$ 。之后生长速率较慢,在  $1\sim 11 \mu\text{m}\cdot\text{a}^{-1}$  之间波动,平均生长速率为  $4.6 \mu\text{m}\cdot\text{a}^{-1}$ 。

利用 220~640 ka B.P. 发育的 5 支石笋年龄数据,结合湖北三宝洞过去 22 万年以来的石笋生长速率数据<sup>[7]</sup>,可以获得 640 ka B.P. 以来三宝洞石笋生长速率变化曲线(图 2, 图 3)。新的结果显示:

(1) 在深海氧同位素(MIS)1, 5.5, 7.5, 9, 15.5 间冰期阶段,石笋生长速率显著增大;相反,冰期阶段石笋生长速率缓慢或者不发育;

(2) 在最近两个间冰期,统计的石笋样本平均生长速率最大,尤其是 MIS5 阶段,最高达约  $600 \mu\text{m}\cdot\text{a}^{-1}$ ;

(3) 石笋生长速率低于  $10 \mu\text{m}\cdot\text{a}^{-1}$  时不能有效地指示冰期—间冰期旋回变化,如 MIS11 和 MIS13 期(图 3)。

表1 三宝洞5支石笋年龄—深度数据\*

Table 1 Age-depth data of 5 stalagmites in Sanbao cave

样号	深度 /mm	年龄 /ka B.P.	年龄误差 /ka	样号	深度 /mm	年龄 /ka B.P.	年龄误差 /ka	样号	深度 /mm	年龄 /ka B.P.	年龄误差 /ka
SB-12	65	425.1	1.1	SB-32	209.5	564.3	5.9	SB-58	870	612.3	5.5
	71	426.2	1.1		215.5	566.0	4.7		901	614.6	5.2
	104	427.3	0.9		220.5	566.9	3.9		922	619.9	5.7
	136	428.4	1.2		226.5	568.9	4.9		948	620.7	5.6
	168	431.1	1.3		234.5	573.9	4.6		972	623.7	5.7
	187	432.0	1.0		290.5	580.9	4.8		977	623.9	6.5
	194	432.3	1.2		298.5	584.2	5.8		977	625.6	9.9
	215	434.4	1.5		332.5	586.0	4.5		1 105	630.3	6.8
	234	434.8	1.1		340.5	588.3	5.4		1 170	638.2	7.4
	272	437.1	1.5		378.5	598.3	6.2		3	426.7	1.25
	299	439.6	1.0		404.5	603.0	6.7		5	427.2	3.0
	362	442.5	1.3		451.5	604.0	6.3		10	428.0	1.7
	372.5	443.1	1.5		459.5	605.5	6.4		14	428.8	1.0
	412	444.7	1.2		493.5	611.6	7.1		40	435.9	1.4
	416	445.5	1.5		509.5	615.3	8.4		57	439.3	2.1
	700	462.7	4.6		537.5	620.3	10.0		94	442.3	1.4
	SB-14	0.3	299.6		3.0	545.5	621.2		6.2	116	443.0
6.2		307.3	3.4	572.5	622.8	6.4	182	446.5	1.3		
8.5		311.3	1.0	8	513.3	2.7	265	452.4	1.3		
8.8		313.1	3.6	13	514.1	3.8	316	453.6	1.4		
10.2		326.9	3.4	20	521.6	2.8	370	455.2	1.8		
12.8		331.8	3.6	27	524.8	3.4	465	459.5	1.8		
13.5		334.8	0.7	43	526.6	2.9	625	464.7	1.9		
19.5		356.8	1.3	50	531.0	3.8	SB-61	102	229.4	0.7	
22.0		364.8	2.9	56	532.7	3.2		141	233.7	1.0	
25.5		370.0	0.9	59	533.4	3.3		161	236.9	0.2	
28.5		375.1	2.9	62	534.5	3.0		193	237.9	0.3	
31.5		385.6	1.2	68	535.7	3.1		243	241.1	0.2	
33.5		391.5	2.7	72	541.5	3.1		291	242.6	0.3	
35.5		396.9	2.8	82	544.8	4.1		311	245.7	0.3	
38.5		402.3	3.5	105	548.7	4.6		330	247.1	0.3	
39.5		402.6	2.3	110	550.7	4.0		366	249.5	0.3	
44.0		403.9	3.9	114	554.6	4.3		394	251.1	0.5	
45.0	406.8	5.0	125	555.6	3.8	413		252.1	0.2		
47.5	409.5	6.0	131	560.8	4.3	423		252.8	0.2		
55.0	417.8	2.1	153	564.8	3.9	495		257.8	0.4		
62.0	422.6	2.0	163	567.7	3.7	519		260.0	0.3		
64.0	425.3	4.4	168	569.2	4.4	553		317.7	0.7		
69.0	432.3	2.1	183	570.6	3.6	571		319.0	0.8		
76.0	445.2	1.8	227	574.3	3.4	623		323.7	0.6		
81.5	462.9	3.3	236	575.7	3.8	742	329.2	0.8			
88.5	473.0	2.4	334	577.3	4.7	847	333.2	1.0			
91.0	478.9	7.8	384	579.8	4.0	960	336.3	0.7			
94.5	483.7	4.5	442	580.6	4.0	1 023	338.9	0.6			
99.5	509.5	7.3	449	582.8	4.5	1 055	341.8	1.0			
109.0	531.8	6.2	495	589.3	5.0	1 143	350.4	0.9			
112.5	532.9	7.0	501	590.9	4.2	1 167	351.9	1.0			
118.5	542.9	5.6	541	593.6	5.1	1 178	354.0	0.8			
122.5	548.7	4.3	547	597.4	5.0	1 291	366.0	1.0			
136.5	551.0	4.4	612	598.5	5.4	1 313	369.5	1.0			
143.5	554.3	4.2	665	605.1	5.6	1 334	372.6	1.2			
157.5	556.0	4.2	705	606.3	5.2	1 361	375.0	0.9			
162.5	556.3	4.5	712	607.0	4.5	1 400	378.8	1.1			
168.5	558.8	3.5	744	607.5	5.1	1 450	383.1	1.3			
177.5	561.0	3.8	784	609.4	6.6	1 452	384.2	1.4			
187.5	561.5	5.4	785	610.1	8.9						

注: \*年龄数值来自文献<sup>[10]</sup>。Note: \*Age value is from literature<sup>[10]</sup>.

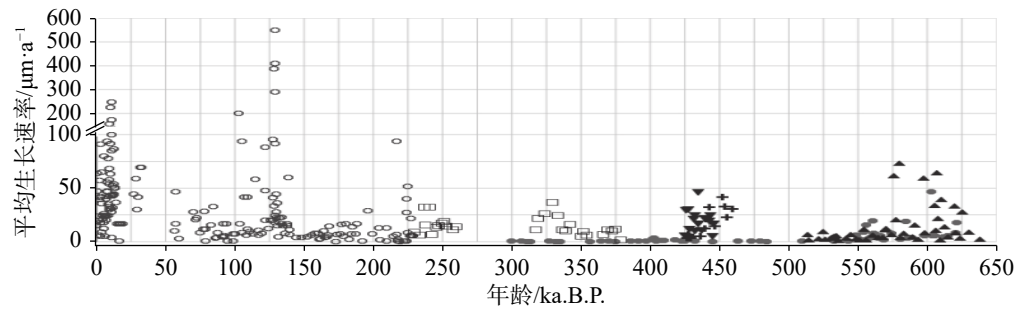


图 2 过去 64 万年三宝洞石笋平均生长速率图

空心圈数据来自文献 [7]

Fig. 2 Average growth rates of stalagmites in Sanbao cave over the past 640 ka B.P.

Hollow ring data is from literature [7]

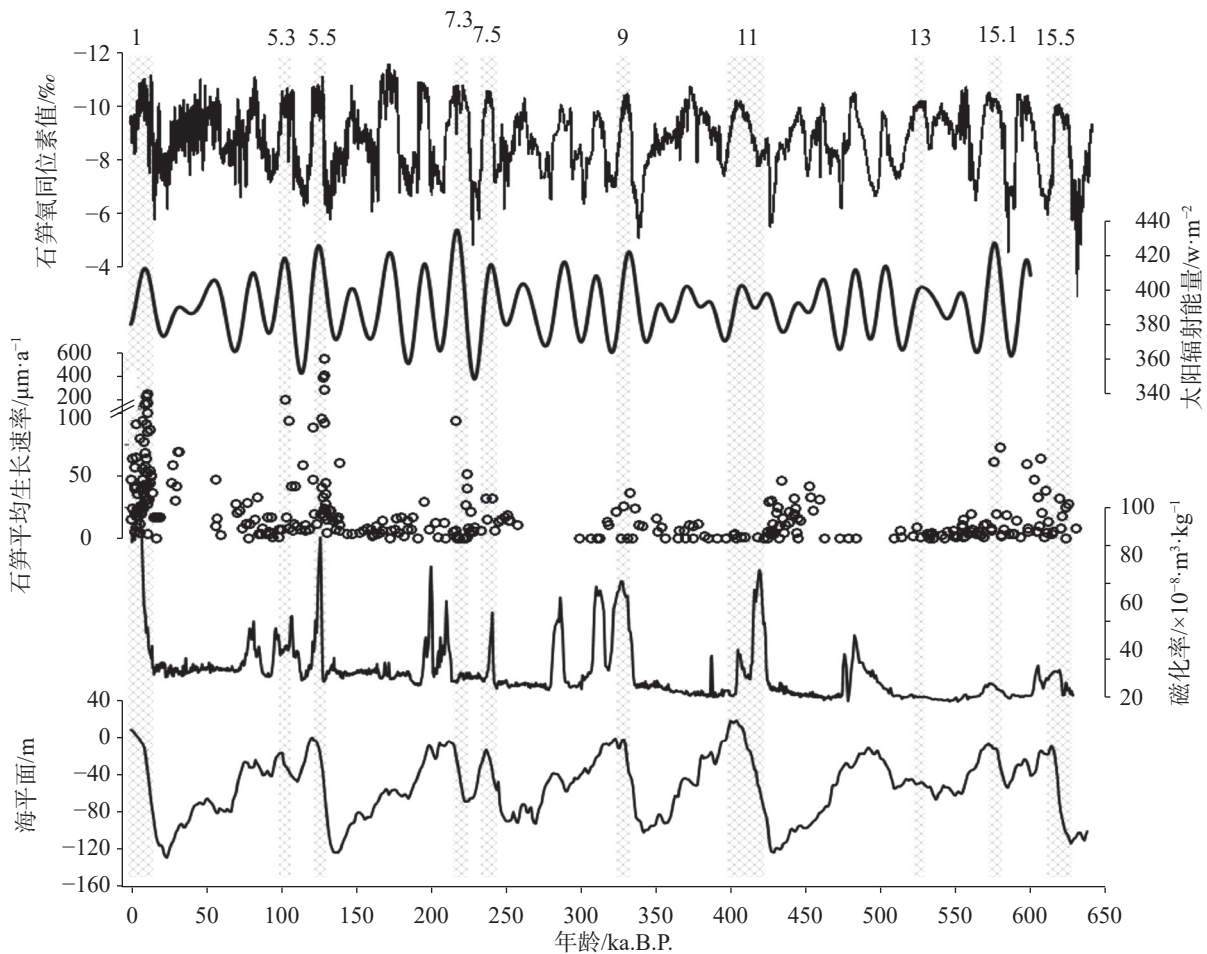


图 3 湖北三宝洞石笋氧同位素记录<sup>[10-11]</sup>、北半球夏季太阳辐射(b)<sup>[12]</sup>、平均生长速率(c)、靖远黄土磁化率记录,其高值表示东亚夏季风强度增强,低值表示东亚夏季风强度减弱(d)<sup>[13]</sup>与海平面记录(e)<sup>[14]</sup>的综合对比(从上至下),图中数字代表深海氧同位素阶段  
Fig. 3 Comparison among stalagmite  $\delta^{18}\text{O}$  record (a)<sup>[10-11]</sup>, insolation in July at 65°N (b)<sup>[12]</sup>, the average growth rate in Hubei Sanbao cave (c), loess magnetic susceptibility record from Jingyuan, Gansu (d)<sup>[13]</sup> and sea level (e)<sup>[14]</sup>

#### 4 讨论

过去二十年来,中国洞穴石笋研究取得了长足的进步,连续重建了过去 64 万年以来具有绝对年龄

控制的古季风演化时间标尺<sup>[10-11, 15-17]</sup>但其  $\delta^{18}\text{O}$  代用指标的指示意义却一直存在争议<sup>[18-24]</sup>。基于现代观察资料、古气候记录以及模式模拟结果,石笋  $\delta^{18}\text{O}$  代用指标在轨道一千年尺度上更可能反映的是一种平均态夏季风强度的变化或者是水汽源—洞穴地点

之间综合水汽输送的结果<sup>[25-28]</sup>。换句话说,在轨道尺度上,石笋  $\delta^{18}\text{O}$  指标所指示地是一个广域性的夏季风强度变化,而不是当地降水量的变化。从这个角度来看,理解洞穴研究点古环境的变化需要结合其它代用指标去相互佐证。石笋沉积速率变化属于一个物理性的气候代用指标,与当地气候要素(尤其是降水和温度)和地下岩溶系统非气候因素密切相关<sup>[6]</sup>。理论上来说,在不考虑具体洞穴环境内部的差异,温暖、湿润的外界环境(类似于间冰期)可能更有利于石笋的沉积,反之亦然<sup>[5-7]</sup>。正如图 3 所示,我们把三宝洞石笋  $\delta^{18}\text{O}$  记录、全球海平面变化、黄土磁化率记录、北半球太阳辐射与统计的洞穴石笋生长速率曲线进行综合对比,结果显示:在过去 6 个间冰期或间冰段,当北半球夏季太阳辐射能量达到高值时,湖北三宝洞石笋生长速率明显增加。例如,在 MIS1, 5.3, 5.5, 7.3, 7.5, 9, 15.1 和 15.5 时期,石笋生长速率显著增加,恰好分别对应于其  $\delta^{18}\text{O}$  记录的偏负时段和黄土磁化率的高值期,指示了亚洲夏季风强度显著增强,当地降水明显增多。然而在过去 6 个冰期,石笋平均生长速率很低,甚至停止生长,对应于黄土磁化率和海平面的低值期。这一结果证实了间冰期暖湿的气候环境更适合石笋高速、连续发育,而冰期干冷的气候环境则抑制其生长发育。而且,在冰期—间冰期转型时,石笋平均生长速率会呈现“爆发式”增长,这说明石笋平均生长速率指标能够敏感地响应不同气候态之间的转型<sup>[7]</sup>。

与  $\delta^{18}\text{O}$  记录不同,统计的三宝洞石笋生长速率在过去几个冰期里呈现出平稳、少变的特点(图 3)。然而,一个例外的情况是:在冰期 MIS12 时段,石笋平均生长速率明显高频增加;相反在间冰期 MIS11 时段,生长速率异常平稳缓慢(图 1)。作者注意到,在冰期 MIS12,三宝洞有 3 支石笋(SB12, SB14 和 SB58)在沉积。与石笋 SB14 低沉积速率记录不同,SB12 和 SB58 在相同生长时段 425—464 ka B.P. 内沉积速率较大,且平均生长速率均超过  $14 \mu\text{m}\cdot\text{a}^{-1}$ 。相反,在间冰期 MIS11,仅有石笋 SB14 在生长,但沉积速率异常低(低于  $1 \mu\text{m}\cdot\text{a}^{-1}$ )。我们认为这种异常的沉积现象(间冰期生长慢,冰期生长快)与洞穴外界气候环境变化无关,可能更多地反映了洞穴内部局地环境的差异,如滴水通道的差异、滴水速率的快慢等因素<sup>[29]</sup>。因此,不难理解生长缓慢的 SB14 生长速率数据为何不能真实地反映冰期—间冰期的变化,以及导致间冰期 MIS11 和 MIS13 缺失(图 2 和图 3)。

从三宝洞 22 支石笋(覆盖过去 64 万年)来看,80% 的石笋平均生长速率呈现出间冰期时期生长快,冰期时期生长慢的特征。这一结果证实石笋平均生长速率代用指标仍能有效指示外部气候环境变化。但是,正如图 3 所示,过去 64 万年以来, MIS5 时期石笋生长速率最快,接近  $600 \mu\text{m}\cdot\text{a}^{-1}$ , MIS1 时期次之,其它间冰期时期石笋生长速率均在  $100 \mu\text{m}\cdot\text{a}^{-1}$  以下。这一特点与石笋  $\delta^{18}\text{O}$  记录有所不同。在过去 6 个间冰期,石笋  $\delta^{18}\text{O}$  值明显偏负,均在  $-11\%$  上下小幅波动,没有显著差异。黄土—古土壤记录<sup>[13,30]</sup> 也表明在最近几个间冰期内,东亚夏季风强度或降水量没有显著差异(图 3d)。因此,考虑受到洞穴内部非气候因素的干扰,认为石笋平均生长速率代用指标仅能定性地指示东亚夏季风强弱的变化。

图 3 所示平均生长速率曲线呈现的冰期—间冰期变化类似于全球海平面和黄土磁化率记录。这种一致性说明了在轨道尺度上,长江中下游地区与华北黄土高原都经历了相似的区域水文条件的变化,这与亚洲夏季风环流强弱变化密切相关<sup>[31]</sup>。在间冰期,高的太阳辐射强度有利于进一步增强海—陆热力差异,导致亚洲夏季风强度明显增强;同时,高的海平面也缩短了水汽的传输距离,进一步放大了夏季风强度的变化,给长江中下游地区和华北地区带来了丰富的降水。这样,在雨—热同期的间冰期或间冰段,暖湿的气候条件有利于地表植被的繁盛、土壤微生物活动增强,致使土壤岩溶水中  $\text{CO}_2$  和  $\text{Ca}^{2+}$  浓度增加,进而导致洞穴沉积物累积的增加<sup>[29]</sup>;相反,在冰期,减弱的太阳辐射可能导致亚洲夏季风强度的减弱;同时,低的海平面增加了水汽源区到研究点的距离,这样使得到达研究区的水汽明显减少,从而导致石笋在冰期沉积缓慢,甚至停止生长。这样,我们初步认为三宝洞沉积速率数据所显示的冰期—间冰期的变化可能归因于全球冰量和太阳辐射共同作用的结果。但个别洞穴,如南京葫芦洞,寒冷的气候条件反而有利于石笋生长,这可能与洞穴的内部沉积环境有关<sup>[3]</sup>。因此,利用石笋生长速率重建古气候历史过程一定要谨慎,尤其是不同洞穴生长速率记录相互对比,获得区域气候变化的共识更需慎重。

## 5 结 论

(1) 基于湖北三宝洞多支石笋平均生长速率数据重建了过去 64 万年以来长江中下游地区东亚夏

季风演化的过程。在间冰期 MIS1, 5.3, 5.5, 7.3, 7.5, 9, 15.1, 15.5 期间, 石笋平均生长速率显著增大, 指示夏季风增强, 区域降水明显增多; 相反, 在冰期阶段 (除了 MIS12 外) 石笋生长速率缓慢或者不发育, 指示夏季风减弱, 降水明显减少。新研究结果进一步证实了石笋平均生长速率代用指标能够有效地指示外部气候环境的变化, 尤其是在冰期—间冰期旋回上;

(2) 在轨道尺度上, 平均生长速率所揭示的冰期—间冰期变化可能归因于全球冰量和太阳辐射共同作用的结果;

(3) 相对于更老的几个间冰期, 最近两个间冰期石笋平均生长速率最大, 尤其是 MIS5 阶段, 这一特征与其它地质记录所重建的结果不同。考虑到洞穴内部非气候因素的影响, 认为石笋生长速率代用指标并不能定量指示夏季风强弱变化。

## 参考文献

- [1] Fleitmann D, Burns S J, Neff U, Mudelsee M, Mangini A, Matter A. Palaeoclimatic interpretation of high-resolution oxygen isotope profiles derived from annually laminated speleothem from Southern Oman[J]. *Quaternary Science Reviews*, 2003, 23(7-8): 935-945.
- [2] Kashiwaya K, Atkinson T, Smart P. Periodic variations in Late Pleistocene speleothem abundance in Britain[J]. *Quaternary Research*, 1991, 35(2): 190-196.
- [3] 邵晓华, 汪永进, 孔兴功, 吴江滢. 南京葫芦洞石笋生长速率及其气候意义讨论[J]. *地理科学*, 2003, 23(3): 304-309.  
SHAO Xiaohua, WANG Yongjin, KONG Xinggong, WU Jiangying. Approach to the growth rate and climatic significance of stalagmites in Hulu Cave, Nanjing[J]. *Scientia Geographica Sinica*, 2003, 23(3): 304-309.
- [4] 林玉石, 张美良, 覃嘉铭, 朱晓燕, 程海. 再论洞穴石笋的沉积速率[J]. *地质论评*, 2005, 51(4): 435-442.  
LIN Yushi, ZHANG Meiliang, QIN Jiaming, ZHU Xiaoyan, CHENG Hai. Growth rate of cave stalagmite[J]. *Geological Review*, 2005, 51(4): 435-442.
- [5] 杨琰, 袁道先, 程海, 覃嘉铭, 林玉石, 张美良, 朱晓燕. 贵州荔波董歌洞较老石笋 ICP-MS  $^{230}\text{Th}$  测年研究及古气候应用[J]. *地层学杂志*, 2008, 32(2): 201-206.  
YANG Yan, YUANG Daoxian, CHENG Hai, QIN Jiaming, LIN Yushi, ZHANG Meiliang, ZHU Xiaoyan. Research on old stalagmites by ICP-MS  $^{230}\text{Th}$  dating and paleoclimate reconstruction in Dongge Cave, Libo, Guizhou[J]. *Journal of Stratigraphy*, 2008, 32(2): 201-206.
- [6] 张美良, 朱晓燕, 李涛, 邹丽霞. 桂林现代洞穴碳酸盐: 石笋的沉积速率及其环境意义[J]. *海洋地质与第四纪地质*, 2011, 31(1): 125-134.  
ZHANG Meiliang, ZHU Xiaoyan, LI Tao, ZOU Lixia. Study on sedimentation rate of modern cave stalagmite carbonate ( $\text{CaCO}_3$ ) deposits and its environmental significance: A case from Panlong Cave, Guilin, China[J]. *Marine Geology & Quaternary Geology*, 2011, 31(1): 125-134.
- [7] 董进国. 湖北三宝洞石笋生长速率及其古气候意义[J]. *第四纪研究*, 2013, 33(1): 146-154.  
DONG Jinguo. The growth and the paleoclimatic significance of stalagmites in Sanbao Cave, Hubei[J]. *Quaternary Sciences*, 2013, 33(1): 146-154.
- [8] 杨琰, 袁道先, 程海. 高精度 ICP-MS  $^{230}\text{Th}$  测年新技术及其在贵州衙门洞 Y1 石笋测年研究中的应用[J]. *中国岩溶*, 2006, 25(2): 89-94.  
YANG Yan, YUAN Daoxian, CHENG Hai. Research on the high precision ICP-MS uranium series  $^{230}\text{Th}$  chronology and a case study on stalagmite Y1 in Yamen Cave, Libo county, Guizhou, China[J]. *Carsologica Sinica*, 2006, 25(2): 89-94.
- [9] 何潇, 王建力, 李清, 李红春, 李廷勇, 程海. 重庆地区石笋沉积速率与古气候意义初探[J]. *中国岩溶*, 2007, 26(3): 196-201.  
HE Xiao, WANG Jianli, LI Qing, LI Hongchun, LI Tingyong, CHENG Hai. Growth rate and the paleoclimatic significance of stalagmites in Chongqing[J]. *Carsologica Sinica*, 2007, 26(3): 196-201.
- [10] Cheng H, Edwards R L, Sinha A, Spötl C, Yi L, Chen S T, Kelly M, Kathayat G, Wang X F, Li X L, Kong X G, Wang Y J, Ning Y F, Zhang H W. The Asian monsoon over the past 640, 000 years and ice age terminations[J]. *Nature*, 2016, 534(7609): 640-646.
- [11] Wang Y J, Cheng H, Edwards R L, Kong X G, Shao X H, Chen S T, Wu J Y, Jiang X Y, Wang X F, An Z S. Millennial- and orbital-scale changes in the East Asian monsoon over the past 22,400 years[J]. *Nature*, 2008, 451(7182): 1090-1093.
- [12] Berger A. Long-term variations of caloric insolation resulting from the Earth's orbital elements[J]. *Quaternary research*, 1978, 9(2): 139-67.
- [13] Sun Y B, Clemens S C, An Z S, Yu Z W. Astronomical timescale and palaeoclimatic implication of stacked 3.6-Myr monsoon records from the Chinese Loess Plateau[J]. *Quaternary Science Reviews*, 2006, 25(1/2): 33-48.
- [14] Spratt R M, Lisiecki L E. A Late Pleistocene sea level stack[J]. *Climate of the Past*, 2016(12): 1079-1092.
- [15] Dong J G, Wang Y J, Cheng H, Hardt B, Edwards R L, Kong X G, Wu J Y, Chen S T, Liu D B, Jiang X Y, Zhao K. A high-resolution stalagmite record of the Holocene East Asian monsoon from Mt Shennongjia, Central China[J]. *The Holocene*, 2010, 20(2): 257-274.
- [16] Cheng H, Edwards R L, Broecker W S, Denton G H, Kong X G, Wang Y J, Zhang R, Wang X F. Ice age terminations[J]. *Science*, 2009, 327: 248-252.
- [17] Wang Y J, Cheng H, Edwards R L, An Z S, Wu J Y, Shen C C,

- Dorale J A. A High-Resolution Absolute-Dated Late Pleistocene Monsoon Record from Hulu Cave, China[J]. *Science*, 2001, 294(5550): 2345-2348.
- [18] Pausata F S R, Battisti D S, Nisancioglu K H, Bitz C M. Chinese stalagmite  $\delta^{18}\text{O}$  controlled by changes in the Indian monsoon during a simulated Heinrich event[J]. *Nature Geoscience*, 2011, 4(7): 474-480.
- [19] Maher B A, Thompson R. Oxygen isotopes from Chinese caves: records not of monsoon rainfall but of circulation regime [J]. *Journal of Quaternary Science*, 2012, 27(6): 615-624.
- [20] Johnson K R, Ingram B L. Spatial and temporal variability in the stable isotope systematics of modern precipitation in China: Implications for paleoclimate reconstructions[J]. *Earth and Planetary Science Letters*, 2004, 220(3-4): 365-377.
- [21] Dayem K E, Molnar P, Battisti D S, Roe G H. Lessons learned from oxygen isotopes in modern precipitation applied to interpretation of speleothem records of paleoclimate from eastern Asia[J]. *Earth and Planetary Science Letters*, 2010, 295(1-2): 219-230.
- [22] Baker A J, Sodemann H, Baldini J U L, Breitenbach S F M, Johnson K R, Hunen J, Zhang P Z. Seasonality of westerly moisture transport in the East Asian summer monsoon and its implications for interpreting precipitation  $\delta^{18}\text{O}$ [J]. *Journal of Geophysical Research: Atmospheres*, 2015, 120(12): 5850-5862.
- [23] Ruan J Y, Zhang H Y, Cai Z Y, Yang X Q, Yin J. Regional controls on daily to interannual variations of precipitation isotope ratios in Southeast China: Implications for paleomonsoon reconstruction[J]. *Earth and Planetary Science Letters*, 2019, 527: 1-8.
- [24] Cai Z, Tian L, Bowen G J. Spatial-seasonal patterns reveal large-scale atmospheric controls on Asian Monsoon precipitation water isotope ratios [J]. *Earth and Planetary Science Letters*, 2018, 503: 158-169.
- [25] 程海, 艾思本, 王先锋, 汪永进, 孔兴功, 袁道先, 张美良, 林玉石, 覃嘉铭, 冉景丞. 中国南方石笋氧同位素记录的重要意义[J]. *第四纪研究*, 2005, 25(2): 157-163.
- CHENG Hai, R L Edwards, WANG Xianfeng, WANG Yongjin, KONG Xinggong, YUAN Daoxian, ZHANG Meiliang, LIN Yushi, QIN Jiaming, RAN Jingcheng. Oxygen isotope records of stalagmites from Southern China[J]. *Quaternary Sciences*, 2005, 25(2): 157-163.
- [26] Cheng H, Edwards R L, Wang Y J, Kong X G, Ming Y F, Kelly M J, Wang X F, Gallup C D, Liu W G. A penultimate glacial-monsoon record from hulu cave and two-phase glacial terminations[J]. *Geology*, 2006, 34: 217-220.
- [27] Cheng H, Sinha A, Wang X F, Cruz F W, Edwards R L. The global paleomonsoon as seen through speleothem records from Asia and the Americas[J]. *Climate Dynamics*, 2012, 39: 1045-1062.
- [28] Zhang H, Brahim Y A, Li H Y, Zhao J Y, Kathayat G, Tian Y, Baker J, Wang J, Zhang F, Ning Y F, Edwards R L, Cheng H. The Asian summer monsoon: Teleconnections and forcing mechanisms—A review from Chinese speleothem  $\delta^{18}\text{O}$  records[J]. *Quaternary*, 2019(2): 26.
- [29] Fairchild I J, Smith C L, Baker A, Fuller L, Spötl C, Mathey D, McDermott F, E I M F. Modification and preservation of environmental signals in speleothems[J]. *Earth Science Reviews*, 2006, 25(1-2): 33-48.
- [30] Beck J W, Zhou W J, Li C, Wu Z K, White L, Xian F, Kong X H, An Z. A 550, 000-year record of East Asian monsoon rainfall from  $^{10}\text{Be}$  in loess[J]. *Science*, 2018, 360(6391): 877-881.
- [31] 王权, 袁莎悦, 梁怡佳, 赵侃, 邵庆丰, 张振球, 朱军吉, 孔兴功, 汪永进, 蓝江湖, 程海, 夏程尉, 李毅. 倒数第三次冰期冰量和太阳辐射对中国东部水文气候的影响[J]. *中国科学: 地球科学*, 2023: 1-10.
- WANG Quan, YUAN Shayue, LING Yijia, ZHAO Kan, SHAO Qingfeng, ZHANG Zhenqiu, ZHU Junji, KONG Xinggong, WANG Yongjin, LAN Jianghu, CHENG HAN, Xia Chengwei, LI Yi. Ice-volume and insolation influences on hydroclimate changes in central eastern China during the antepenultimate glacial period[J]. *Science China Earth Sciences*, 2023: 1-10.

## Variation of stalagmite growth rate and its paleoclimatic significance in Sanbao cave, Hubei Province over the past 640,000 years

JIANG Ying<sup>1,2</sup>, WEI Wei<sup>1</sup>, FENG Xiaoyi<sup>1</sup>, ZHANG Han<sup>1</sup>, ZHU He<sup>1</sup>, DONG Jinguo<sup>1</sup>

(1. College of Geography Science, Nantong University, Nantong, Jiangsu 226006, China; 2. College of Geography Science, Nanjing Normal University, Nanjing, Jiangsu 210023, China)

**Abstract** In the past few decades, great progress has been made in the study of stalagmite paleoclimate. Compared with the geochemical indicators such as stalagmite  $\delta^{18}\text{O}$ , the average growth rate of stalagmite is a physical indicator, which can directly reflect the wet and dry changes of the external climate, and is one of the important means to reconstruct the past regional hydrological changes.

Sanbao cave (31°40'N, 110°27'E), the study area, is located in Shennongjia National Nature Reserve, Hubei Province, on the north bank of the Three Gorges of the Yangtze River and adjacent to the southern edge of the Loess

Plateau. Mainly affected by the East Asian summer monsoon, the average annual temperature in this area is 8-9°C with the annual precipitation of 2,000 mm. In summer, warm and humid air from the equatorial ocean enters the hinterland of the mainland, bringing about 60% of the annual precipitation. In winter, the dry and cold air from Siberia controls the climate in Shennongjia area, so it is particularly sensitive to the seasonal advance and retreat of East Asian summer monsoon. Sanbao cave, 1,900 m above sea level, is located on the northern slope of Shennongjia Mountain in Hubei Province, covered with limestone layer about 300 m thick. The thickness of the surface layer is about 2-3 m, mainly distributed with trees, shrubs and weeds. The research objects are five stalagmites (numbered SB12, SB14, SB32, SB58 and SB61) from Sanbao Cave, with a cumulative height of about 2.991 m, of which SB61 was deposited in 229.4-384 ka B.P., corresponding to MIS8-MIS10; SB14 grew and developed from 299.6-622.8 ka B.P., spanning from MIS9 to MIS15; SB12 and SB58 were respectively deposited at 425.1-462.7 ka B.P. and 426.7-464.7 ka B.P., corresponding to MIS12; SB32 grew from 514.3-638.2 ka B.P., and spanned from MIS13 to MIS15.  $^{167}\text{230Th}$  age data of these five stalagmites was obtained by the analytical instruments of Thermo-Finnigan Element and Thermo-Finnigan Neptune in Minnesota Isotope Laboratory, the USA. The age analysis error was  $\pm 2\sigma$  measurement statistical error with the error accuracy of 0.5-2.0 ka. For the calculation of average growth rates of stalagmites, firstly, the data of stalagmite age reversal in stratigraphy has been excluded. Then, the curve of the measured age point of stalagmite and its corresponding growth depth has been established. The new results are basically consistent with the growth rate curve in the original literature. Finally, the average growth rates of stalagmites have been obtained by dividing the depth difference between two adjacent points by the measured age difference.

Based on  $^{167}\text{230Th}$  age data from 5 stalagmites spanning 220,000 to 640,000 years in Sanbao cave, and combined with the past work, this paper has reconstructed the precipitation change process of East Asian summer monsoon (EASM) in the middle and lower reaches of the Yangtze River over the past 640,000 years in the late Pleistocene. The results show that the growth rates of stalagmites in Marine Isotope Stages (MIS) 1, 5.3, 5.5, 7.3, 7.5, 9, 15.1, 15.5 increased significantly, indicating that the intensity of EASM increased significantly with more precipitation in the interglacial stage. On the contrary, the slow or undeveloped growth rates in the glacial stage indicate the weakening of the summer monsoon intensity with less precipitation. Based on statistical analysis of the growth rates of 22 stalagmites, we hold that the average growth rate index cannot quantitatively indicate the change of the monsoon intensity. Moreover, when the stalagmite growth rate is less than  $10\ \mu\text{m}\cdot\text{a}^{-1}$ , it also cannot effectively indicate the glacial-interglacial change. On the orbital scale, the glacial-interglacial fluctuation revealed by the average growth rate may be attributed to the joint action of global ice and solar radiation.

Finally, it should be noted that in different time scales, the controlling factors of stalagmite growth rate are complicated, and the noise generated by the environment difference inside the cave may cover up or weaken the transmission of the climate signal from the outside to the inside. Therefore, the possible influencing factors must be carefully considered when we reconstruct the paleoenvironment by using the average growth rates of stalagmites.

**Key words** stalagmite, growth rate, glacial-interglacial period, East Asian summer monsoon, Sanbao cave, Hubei

(编辑 张玲)